

Stability Analysis of a Vision-Based Control Design for an Autonomous Mobile Robot*

J.B. Coulaud, G. Champion, G. Bastin, and M. De Wan
 UCL-CESAME, Av G. Lemaître, 4-6, B1348
 Louvain-La-Neuve, Belgium, coulaud@inma.ucl.ac.be
 SHORT PAPER

Abstract—We propose a simple control design allowing a mobile robot equipped with a camera to track a line on the ground. The control algorithm as well as the image processing algorithm are very simple. We discuss the existence and the practical stability of an equilibrium trajectory of the robot when tracking a circular reference line. We then give a complementary analysis for arbitrary reference lines with bounded curvature. Experimental results confirm the theoretical analysis.

Index Terms—mobile robot, control design analysis, visual-servoing, path tracking

I. INTRODUCTION

The problem addressed in this paper is the feedback control design allowing a mobile robot to track a line on the ground using a visual feedback. There exist a lot of image processing algorithms extracting a map of the environment from the data provided by a camera (see for instance [1]- [4]). But the implementation of such sophisticated algorithms is quite complex. On the other hand, there exist several approaches to design a control allowing to track a reference trajectory (see [5]- [10]). For instance, the differential flatness of the robot allows to reduce the problem to a path planning problem (see [11]- [13]). But these approaches require a highly accurate on-line extraction of the line shape. Another interesting approach is presented in [14]: instead of considering separately the estimation from the vision measurements and the design of control strategies, the authors formulate the tracking problem as one of controlling directly the shape of the curve in the image plane. The practical implementation is however rather sophisticated, implying an extended Kalman filter to dynamically estimate the image parameters required for the feedback control.

Our purpose in this paper is to propose a simple solution of this tracking problem which avoids as much as possible sophisticated image processing and control algorithms. The practical implementation is straightforward and can easily be achieved on line. Our main contribution is to provide a complete stability analysis of the control system, taking into account a restriction on the field of view. Restricting ourselves, in a first step, to a particular reference trajectory (a circle) we discuss the conditions of existence of a stable equilibrium trajectory of the robot with respect to the line, and, analysing the phase plane, we explicit the domain of attraction of this equilibrium. Then, in a second step, the discussion is extended to reference lines with arbitrary shape. This analysis provides, together with the convergence conditions, guidelines allowing the user to calibrate and adapt the design parameters of the control law in order to ensure better closed-loop performance.

*This paper presents research results of the Belgian Programme on Interuniversity Attraction Poles, initiated by the Belgian Federal Science Policy Office. The scientific responsibility rests with its authors.

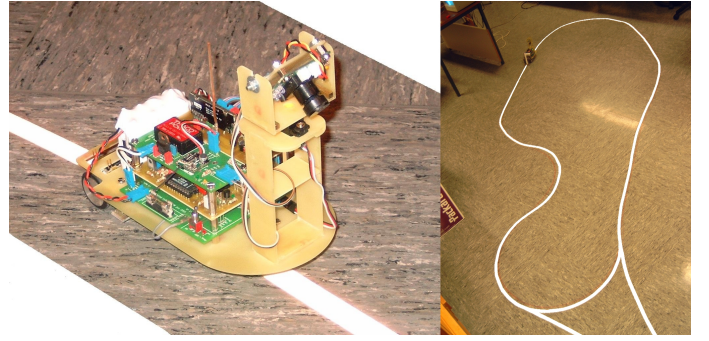


Fig. 1. The experimental robot and a test path

We first describe the experimental device (Section II) and then derive the robot kinematic model and the control design (Section III). Section IV is devoted to the existence and stability of an equilibrium trajectory around a circular line, and the behavior of the system for arbitrary reference line with upper bounded curvature. Finally, we show, with an example, how this simple design can be easily extended by a dynamical assignment of the parameters (Section V). Sections IV and V are illustrated with experimental results.

II. DESCRIPTION OF THE ROBOT

The mobile robot is of unicycle type: it has two fixed wheels at the back and a caster wheel at the front, which has no influence on the kinematic properties. The length of the robot is 22cm and the distance between the fixed wheels is 7.4cm.

The vision device is constituted by a monochromatic camera with a resolution of 320×240 . It is fixed on the robot, at a height of 17cm, at a distance of 14.2cm from the rear axle. It leans forward, with an angle of 45° . The lateral angle of view is 60° , which limits significantly the field of view. Image data are transmitted to a computer via an analogical video interface PAL to USB2.0.

The control is achieved by the computer which processes the data transmitted by the vision device, in order to provide the speed control for the two fixed wheels, according to the feedback control law.

III. KINEMATIC MODEL AND CONTROL DESIGN

We suppose - as it is usually done - that the contact between the wheel and the ground satisfies both conditions of *pure rolling* and *non-slipping* during the motion; moreover the robot is assumed to be rigid.

With these assumptions we have the well known kinematic model:

$$\begin{aligned} \dot{x} &= v \cos \theta \\ \dot{y} &= v \sin \theta \\ \dot{\theta} &= \omega \end{aligned} \quad (1)$$

where (x, y) denote the coordinates of the middle point P of the rear axle, θ is the angle that specifies the robot orientation in a reference frame $(0, \vec{x}_0, \vec{y}_0)$ linked to the ground, v is the linear velocity of P (also called forward velocity) and ω is the angular velocity. The velocities v and ω can be assigned by the physical inputs of the experimental device, *i.e.* the rotation speeds of the two fixed wheels.

Our control strategy is quite natural: essentially it consists in controlling the orientation so that the path to track would be centered in the field of view. This control design is particularly suited for the considered vision device: a visual sensor directed ahead with a limited field of view.

We define the *horizon* as the straight line on the ground which is parallel to the rear axle, at a distance H ahead from it (see Fig.2). We then consider P_r , the intersection point between the horizon and the line to track. If the curvature of the line is not too strong, this point is unique. In case of multiple intersection points, P_r will be the closest to the robot longitudinal axis. We define Z as the distance between P_r and the longitudinal axis.

Z can be easily extracted from the pictures provided by the vision system. The horizon corresponds in these pictures to a row of pixels, while P_r corresponds to the intersection of this row with the image of the line on the ground (see Fig. 3). The distance Z is proportional to the number of pixels between the middle point of this row and the image of P_r ¹.

The control law is defined as follows:

- the forward velocity is imposed to be constant: $v = v_0$
- the angular velocity is proportional to Z : $\omega = kZ$, with k constant.

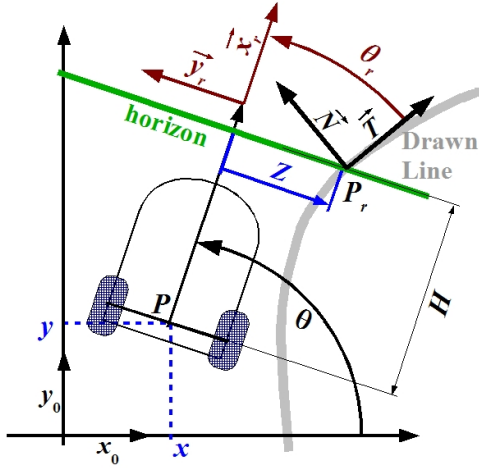


Fig. 2. Control Principle

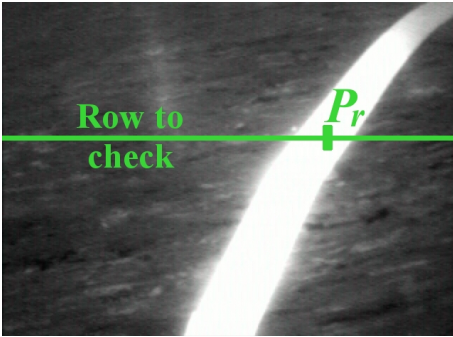


Fig. 3. Extracting the target point from the data

¹Assuming that distortion effects can be neglected, as H is constant, there is a single proportionality coefficient to evaluate in a calibration phase in order to obtain Z from the image measurement.

The resulting closed loop system is then described by the following equations:

$$\begin{aligned}\dot{x} &= v_0 \cos \theta \\ \dot{y} &= v_0 \sin \theta \\ \dot{\theta} &= kZ\end{aligned}\quad (2)$$

State variables x , y and θ are not relevant to analyze the convergence properties of the system: variables describing the position of the robot with respect to the line would be preferable.

We define the Frenet reference frame of the tracked line at the target point P_r : (P_r, \vec{T}, \vec{N}) , and we introduce the following variables:

- θ_r the angle (\vec{T}, \vec{x}_r) ,
- $S(t)$ the curvilinear coordinate of P_r ,
- $c(t)$ the curvature of the path at P_r ,
- θ_c the angle (\vec{x}_0, \vec{T}) .

We can see that, as soon as there is an intersection between the horizon and the path to follow:

$$P_r(S(t)) = P(t) + H\vec{x}_r(\theta(t)) + Z(t)\vec{y}_r(\theta(t))$$

Differentiating this expression we obtain:

$$\dot{S}\vec{T}(S) = v\vec{x}_r + H\dot{\theta}\vec{y}_r - Z(t)\dot{\theta}\vec{x}_r + \dot{Z}\vec{y}_r$$

Projecting this equation on the Frenet frame, and including the feedback control law (2) we have:

$$\begin{aligned}\dot{Z} &= -kHZ + (kZ^2 - v) \tan \theta_r \\ \dot{S} &= \frac{v - kZ^2}{\cos \theta_r}\end{aligned}$$

Moreover: $\dot{\theta}_r = \dot{\theta} - \dot{\theta}_c$ which leads to

$$\dot{\theta}_r = kZ - \dot{S}c(S)$$

where $c(S)$ is the curvature of the path. Then the system can be described as follows:

$$\begin{aligned}\dot{Z} &= -kHZ - (v - kZ^2) \tan \theta_r \\ \dot{\theta}_r &= kZ - c \frac{v - kZ^2}{\cos \theta_r}\end{aligned}\quad (3)$$

with c satisfying the following equation:

$$\dot{c} = \frac{dc}{dS} \frac{v - kZ^2}{\cos \theta_r}\quad (4)$$

Defining non dimensional time $\tau = Hkt$ and variables

$$z = \frac{Z}{H}, \quad u = \sin(\theta_r), \quad s = \frac{S}{H}, \quad \sigma = Hc, \quad \varpi = \frac{v}{kH^2}, \quad (5)$$

equations (3) and (4) can be rewritten as:

$$\begin{aligned}\frac{dz}{d\tau} &= -z - (\varpi - z^2) \frac{u}{\sqrt{1-u^2}} \\ \frac{du}{d\tau} &= z\sqrt{1-u^2} - \sigma(\varpi - z^2) \\ \frac{d\sigma}{d\tau} &= \frac{d\sigma}{ds} \frac{\varpi - z^2}{\sqrt{1-u^2}}\end{aligned}\quad (6)$$

In other words, if the time unit is $\tau_0 = \frac{1}{kH}$ and the length unit is H , then τ represents the time, z the deviation, σ the curvature, s the curvilinear abscissa, and ϖ the velocity of the robot. The advantage of this new system is to make clear that the behaviors of z and u essentially depend on σ and ϖ .

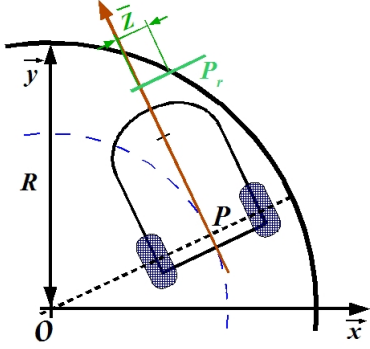


Fig. 4. Circle tracking

IV. STABILITY ANALYSIS

A. Equilibrium trajectory for a circular line

In this section we consider the particular case when the line on the ground is a circle centered at O , the origin of the Galilean reference frame, with radius $R = \frac{1}{c}$, as shown in Fig.4. Here, c , v_0 , H and k are constant parameters. Therefore the system is described by the first two equations of (6) where pseudo curvature σ and pseudo velocity ϖ have constant values.

1) Local stability of the equilibrium:

We first characterize the equilibrium trajectory of the robot with respect to the circle and then discuss the conditions of stability of this equilibrium. An equilibrium corresponds to constant values of the variables z and u , denoted $(\bar{z}$ and $\bar{u})$ implying that P , the middle point of the rear axle, describes itself a circle with the same center.

We must consider several constraints on variables z and u :

- u is naturally bounded: $|u| \leq 1$
- The proposed control design will fail if the center of the circle belongs to the longitudinal axis of the robot: in this case, there are either two target points equidistant from the robot axle, or no target point. When $\sigma \geq 0$ (in this case the robot runs counter-clockwise) this implies that:

$$\sigma z + \sqrt{1 - u^2} > 0 \quad (7)$$

With these constraints on values of (z, u) , there is only one equilibrium point given by:

$$\begin{aligned} \bar{z} &= \frac{1}{2\sigma} (\sqrt{1 - \sigma^2} + 4\sigma^2 \varpi - \sqrt{1 - \sigma^2}) \\ \bar{u} &= -\sigma \end{aligned} \quad (8)$$

But this equilibrium point corresponds to an admissible situation only if the target point remains in the field of view. This condition introduces an upper bound for the admissible values of z , z_{max} , which depends on the horizon H and the camera view angle. An equilibrium is therefore admissible if $|\bar{z}| \leq z_{max}$. Equation (8) implies that $\bar{z} \leq \sqrt{\varpi}$.

- 1) Then, if $z_{max} \geq \sqrt{\varpi}$, the equilibrium is admissible as soon as the pseudo curvature satisfies $\sigma \leq \sigma_{max} = 1$.
- 2) If $z_{max} \leq \sqrt{\varpi}$, it can be checked that the condition $|\bar{z}| \leq z_{max}$ is satisfied only if

$$\sigma \leq \sigma_{max} = \frac{z_{max}}{\sqrt{z_{max}^2 + (\varpi - z_{max}^2)^2}}$$

The two cases are summarized by the following inequality:

$$R > \frac{H}{\sigma_{max}} \geq H \quad \text{with the adequate } \sigma_{max}(z_{max}) \quad (9)$$

The Jacobian matrix of the system (z, u) around (\bar{z}, \bar{u}) is:

$$\begin{pmatrix} -\sqrt{1 + \frac{4\sigma^2 \varpi^2}{1 - \sigma^2}} & \frac{\sqrt{1 - \sigma^2} - \sqrt{1 - \sigma^2 + 4\sigma^2 \varpi^2}}{2\sigma^2(1 - \sigma^2)} \\ \sqrt{1 - \sigma^2 + 4\sigma^2 \varpi^2} & \frac{1}{2} (\sqrt{1 + \frac{4\sigma^2 \varpi^2}{1 - \sigma^2}} - 1) \end{pmatrix} \quad (10)$$

The eigenvalues of this matrix have always a negative real part, which implies that the system is locally asymptotically stable around the state given by (8).

2) Phase plane analysis:

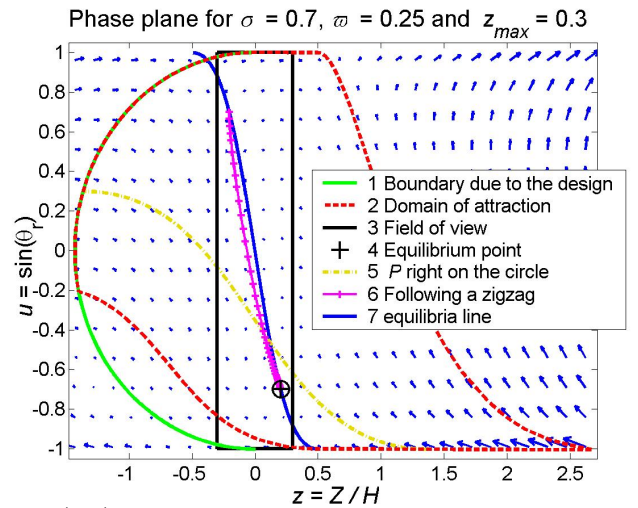
We now represent in the phase plane (z, u) the results of a more detailed analysis, for a pseudo curvature $\sigma = 0.7$ corresponding to a radius $R = \frac{10}{7}H$.

In Fig.5, we represent the physical boundaries corresponding to the constraints $|z| < z_{max}$ and $|u| < 1$ (box n°3).

Then depending on the value of the pseudo curvature σ , we represent the following informations:

- 1) The boundary (curve 1) induced by equation (7) corresponding to the inadmissible position of the robot with respect to the circle.
- 2) The vector field (arrows) defined by equation (6).
- 3) The equilibrium point (n°4); it belongs to the line number 7 representing all equilibrium points.
- 4) The boundary (n°2) of the domain of attraction without considering constraints.
- 5) Number 6 is an example of trajectory.

The *practical domain of attraction* is the largest stable attractive area included in the intersection of the black rectangle (n°3) with the area bounded by the dashed line (n°2). We can observe by numerical computations that the previous intersection itself is in fact a good approximation of the *practical domain of attraction*.

Fig. 5. (z, u) phase plane

We denote Δ the distance from O to P , and δ the corresponding non dimensional variable $\delta = \frac{\Delta}{H}$; then:

$$\delta = \sqrt{\left(z - \frac{\sqrt{1 - u^2}}{\sigma}\right)^2 + \left(1 + \frac{u}{\sigma}\right)^2}$$

The set for which the point P is right on the line to follow is defined by $\Delta = \frac{1}{c}$ or equivalently $\delta = \frac{1}{\sigma}$ and corresponds to the equation:

$$z = \frac{1}{\sigma}(\sqrt{1 - (u + \sigma)^2} - \sqrt{1 - u^2}) \quad (11)$$

It is the curve n°5 on the figure. We can see that this curve separates the plane phase in two regions: the first one contains the states for which P is inside the circle, and the other one the states for which P is outside.

It can be interesting to give a kind of *stability margin* m_s for this system. A good estimator is the distance in the phase plane, between the equilibrium and the boundary of the *practical domain of attraction*. This is actually the distance between the equilibrium point and the black rectangle boundary in the phase plane. A possible way to measure is be the following definition:

$$m_s = \sigma_{max} - \sigma \quad (12)$$

where σ_{max} is the same as in inequality (9).

This m_s must be positive and the robustness of the design increases with it. A pretty good choice is to require $m_s \geq 0.3$ which will be done in the following sections. This leads to a practical upper bound for σ denoted σ_p

3) Convergence rate:

Another interesting point is the time necessary to converge to the equilibrium trajectory.

From a physical point of view, the relevant variable for convergence is z , because the control design can be applied only if the line is in the field of view. Then we choose the distance $d = |z - \bar{z}|$ to define a convergence criterion, even if it does not take into account the other state variable u . The system is considered to be close enough to the equilibrium when $d < 0.05$. Let us denote $D(z_0, u_0)$ the distance traveled by P from the initial state (z_0, u_0) till the trajectory reaches the region where $d < 0.05$.

The problem has been investigated by systematical simulations of trajectories of the system (6). The set of parameters for the pseudo curvature σ and the pseudo velocity ϖ is: $\mathcal{D} = \{(\sigma, \varpi) \in]0, 0.7] \times \{\frac{1}{4}\}\}$. The set of initial states (u_0, z_0) is the boundary of the domain of attraction (n°2 in Fig.5). For all the simulations we observe that: $D < D_{max} = 3H$

This means that, whatever the admissible initial state, the robot is very close to the equilibrium after a traveled distance less than $D_{max} = 3H$ which is a quite good speed of convergence compared with the size of the robot.

4) Experimental results:

The reference line is circle of radius $R=40\text{cm}$. Unfortunately, the drawing of the line is corrupted by local disturbances resulting in fluctuations in the curvature along the line. In our experiment $v_0 = 20\text{cm/s}$, $k = 18$ and $H = 35\text{cm}$. So $\sigma = \frac{H}{R} \approx 0.875$ and $\sqrt{\varpi} = \sqrt{\frac{v_0}{kH^2}} \approx 0.30$. We also have $Z_{max} = 7.5\text{cm}$, so $z_{max} = \frac{Z_{max}}{H} \approx 0.21$, which leads to $\sigma_{max} \approx 0.98$ which satisfies (9).

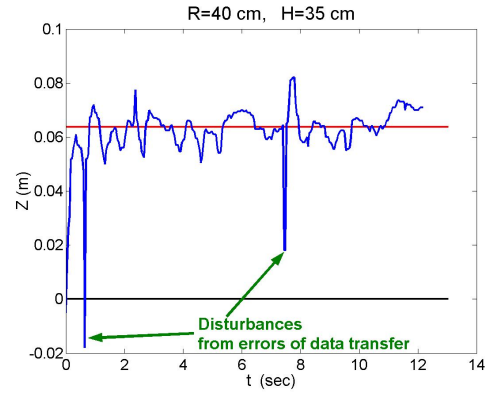


Fig. 6. $Z(t)$ in mm while tracking a circle with a radius of 40 cm, at $v_0 = 0.20$ m/s and $k = 18$

We represent in Fig.6 the evolution of the variable Z , involved in the feedback control. As expected from the above analysis the variable Z converges asymptotically to a steady-state value. The oscillations around the steady state-value result from the curvature irregularities and from interferences in the transmission of the data (the 2 peaks appearing in the record).

B. Extension to arbitrary curves

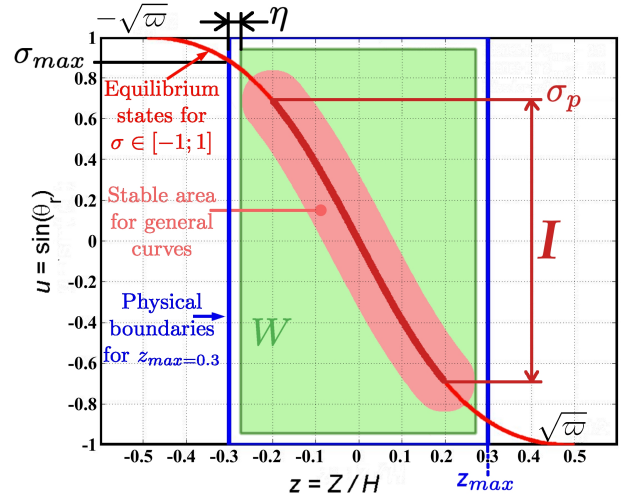


Fig. 7. Admissible radii for $\varpi = 0.25$

In the previous section, we have analyzed the stability when the robot tracks a circular path. In this section, we will consider the tracking of a path having an arbitrary (smooth) curvature.

A natural question is the following: *if the line to track is such that its curvature satisfies relation (9) at every point, will the robot follow this trajectory?*

We study this problem in two steps:

- first, we give a mathematical point of view which proves that under some assumption on $\frac{dc}{ds}$, the answer to the previous question is affirmative.
- then we give a complementary numerical study of a particular curve hard to track. This leads to some conclusions about the orders of magnitude of the boundaries we have to impose on the parameters.

1) *Theoretical analysis:*

This section establishes a formal result, which support the conclusions of the next paragraph. System (6) is shown to be a *slowly varying system* that fulfills assumptions of a theorem given in [15], provided that $|\frac{dc}{ds}|$ has an appropriate upper bound.

Proposition. If the line to be tracked has a continuously differentiable pseudo curvature $\sigma(s) = Hc(s)$ s.t.

- (i) $|\sigma| \leq \sigma_p$,
- (ii) $\exists \epsilon > 0, \quad |\frac{d\sigma}{ds}| \leq \epsilon$

then for sufficiently small ϵ and tracking error at the initial conditions, the tracking error is uniformly bounded.

Proof. Let us define the function f s.t. system (6) is rewritten as

$$\dot{w} = f(w, \sigma)$$

As stated in equations (8), for each value of $\sigma \in I$, there exists an equilibrium $\bar{w} = (\bar{z}, \bar{u})$; this defines a function h :

$$\bar{w} = h(\sigma) \Leftrightarrow f(h(\sigma), \sigma) = 0$$

For each τ we define the deviation from the equilibrium corresponding to $\sigma(\tau)$:

$$\tilde{w}(\tau) = w(\tau) - h(\sigma(\tau))$$

Our purpose is to show that \tilde{w} is upper bounded.

The evolution of \tilde{w} is described by the following equation:

$$\frac{d\tilde{w}}{d\tau} = g(\tilde{w}, \sigma) - \frac{dh}{d\sigma} \frac{d\sigma}{d\tau}$$

where $g(\tilde{w}, \sigma) = f(h(\sigma) + \tilde{w}, \sigma)$.

We know that for a constant value of σ , $\tilde{w} = 0$ is an exponentially stable equilibrium. Let us consider the following Lyapunov function corresponding to a fixed value of σ :

$$V(\tilde{w}, \sigma) = \tilde{w}^T P(\sigma) \tilde{w}$$

In this expression $P(\sigma)$ is the solution of the Lyapunov equation:

$$J(\sigma)^T P(\sigma) + P(\sigma) J(\sigma) = -Id$$

where $J(\sigma)$ is the Jacobian of $g(\tilde{w}, \sigma)$ evaluated at $\tilde{w} = 0$:

$$J(\sigma) = \frac{\partial g}{\partial \tilde{w}}(0, \sigma)$$

$P(\sigma)$ is continuously differentiable and definite positive.

We define the following constants

$$\begin{aligned} A_1 &= \min_{\sigma \in I} \min_{\lambda \in Sp(P)} \lambda \\ A_2 &= \max_{\sigma \in I} \max_{\lambda \in Sp(P)} \lambda \\ A_4 &= 2A_2 \\ A_5 &= \max_{\sigma \in I} \max_{\lambda \in Sp(\frac{\partial P}{\partial \sigma})} |\lambda| \\ L &= \max_{\sigma \in I} (\|\frac{dh}{d\sigma}\|) \end{aligned}$$

where $Sp(M)$ is the set of eigenvalues of the matrix M .

We define in the (z, u) plane a compact set W (the rectangle in Fig.7):

$$W = [-z_{max} + \eta, z_{max} - \eta] \times [-1 + \eta, 1 - \eta]$$

with $\eta > 0$ a small constant, such that for each $\sigma \in I$, $h(\sigma)$ is in the interior of W . We denote:

$$A_0 = \max_{w \in W} \left| \frac{\varpi - z^2}{\sqrt{(1-u^2)}} \right|$$

It is then possible to define $r_1 > 0$ such that each ball $B(h(\sigma), r_1)$ is included in W .

We are now able to define a constant B such that $\forall \sigma \in I, \forall \tilde{w} \in B(0, r_1)$:

$$\begin{aligned} \|\frac{\partial V}{\partial \sigma}\| &\leq A_5 \|\tilde{w}\|^2 \\ \|g(\tilde{w}, \sigma) - J(\sigma)\tilde{w}\| &\leq B \|\tilde{w}\|^2 \\ \|\frac{\partial V}{\partial \tilde{w}}\| &\leq 2A_2 \|\tilde{w}\| \\ \|\frac{d\sigma}{d\tau}\| &\leq A_0 \|\frac{d\sigma}{ds}\| \leq A_0 \epsilon \end{aligned}$$

We conclude that for $\sigma \in I$ and $\tilde{w} \in B(0, r_1)$:

$$\begin{aligned} \frac{\partial V}{\partial \tilde{w}} g(\tilde{w}, \sigma) &= \frac{\partial V}{\partial \tilde{w}} J(\sigma) \tilde{w} + \frac{\partial V}{\partial \tilde{w}} (g(\tilde{w}, \sigma) - J(\sigma) \tilde{w}) \\ &= -\|\tilde{w}\|^2 + \frac{\partial V}{\partial \tilde{w}} (g(\tilde{w}, \sigma) - J(\sigma) \tilde{w}) \\ &\leq -\|\tilde{w}\|^2 + \|\frac{\partial V}{\partial \tilde{w}}\| B \|\tilde{w}\|^2 \\ &\leq (-1 + 2A_2 B \|\tilde{w}\|) \|\tilde{w}\|^2 \end{aligned}$$

So, for any $A_3 \in (0, 1)$ there exists $r \in (0, r_1]$ such that $\forall \sigma \in I, \forall \tilde{w} \in B(0, r)$,

$$\frac{\partial V}{\partial \tilde{w}} g(\tilde{w}, \sigma) \leq -A_3 \|\tilde{w}\|^2 \quad (13)$$

The five hypotheses of Theorem 5.5 in Chapter 5 of [15] are therefore satisfied for $\sigma \in I$ and $\tilde{w} \in B(0, r)$ (the corresponding domain is represented by the stripe around the line of all equilibria):

- 1) $\|\frac{dh}{d\sigma}\| \leq L$
- 2) $\forall \sigma \in I, A_1 \|\tilde{w}\|^2 \leq V(\tilde{w}, \sigma) \leq A_2 \|\tilde{w}\|^2$
- 3) $\forall \sigma \in I, \|\frac{\partial V}{\partial \tilde{w}}\| \leq A_4 \|\tilde{w}\|$
- 4) $\forall \sigma \in I, \|\frac{\partial V}{\partial \sigma}\| \leq A_5 \|\tilde{w}\|^2$
- 5) $\|\frac{\partial V}{\partial \tilde{w}} g\| \leq -A_3 \|\tilde{w}\|^2$

Under these conditions, Theorem 5.5 in [15] gives the following conclusions:

- 1) There exists $\epsilon_{max} > 0$, such that, if $\|\tilde{w}(0)\| < r \sqrt{\frac{A_1}{A_2}}$ and $\|\frac{d\sigma}{ds}\| \leq \epsilon < \epsilon_{max}$, then the solutions of the system for $t \geq 0$ are uniformly bounded.
- 2) Moreover solutions are also uniformly ultimately bounded with a bound $b = \frac{A_0 A_2 A_4 L \epsilon}{\theta (A_1 A_3 - \epsilon A_2 A_5)}$, for every $\theta \in (0, 1)$.

□

2) Tracking a zigzag:

We illustrate this stability discussion by considering a particular curve which is a sequence of two arcs of circles with an intermediate inflexion point as shown in Fig.8. Intuitively this curve seems difficult to track because it has not a differentiable curvature. Nevertheless, a numerical simulation shows that it does not matter actually. The radii of the two circles are chosen equal to $R = \frac{1}{c_{max}} = \frac{1}{H\sigma_p}$ corresponding to $\sigma_p = 0.7$. Moreover:

$$(\sigma, \varpi) \in \mathcal{D} \quad (14)$$

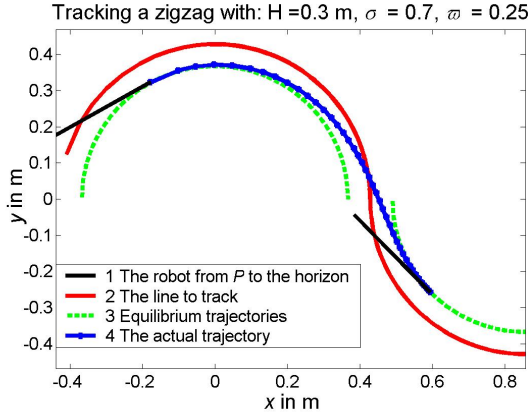


Fig. 8. A difficult line to track

The robot is initially stabilized on the first arc equilibrium trajectory and we want to know if it will join the equilibrium trajectory of the second arc. We can look again at Fig.5 where the trajectory n°4 represents this transition. It is important to note that the whole trajectory is in the field of view, *i.e.* $|z| \leq z_{max}$.

Furthermore, if we evaluate again a stabilizing distance D at $d < 0.05$ for this particular trajectory, we find a value less than $2H$.

We can then draw the following conclusions: if

- 1) parameters satisfy equation (14)
- 2) stability margin $m_s \geq 0.3$ everywhere
- 3) two successive inflexion points M and N are always

$$\text{such that: } \widehat{MN} > D_{max} = 3H$$

then the robot will be able to track this line.

We now can give a consistent numerical value for ϵ_{max} (the upper bound of $\frac{d\sigma}{ds}$) from the simulation of the zigzag tracking:

$\widehat{MN} > D_{max}$ for two successive inflexion points M and N , can be strengthened in

$$\left| \frac{d\sigma}{ds} \right| \leq \epsilon_{max} = \frac{\sigma_p H}{D_{max}} \quad (15)$$

V. TAKING ADVANTAGE OF THE ANALYSIS

A. Select the equilibrium trajectory when tracking a circle

The discussion presented in section IV-A.1 has show how the design parameters influence the equilibrium trajectory when tracking a circular line. We can therefore take advantage

of equations (8) to adapt the parameters σ and ϖ so that the circular equilibrium trajectory has a desired position. This adaptation is possible since σ and ϖ are functions of physical parameters v_0 , k and H , at the user choice. For example, it is possible to make the tracked circle itself to be the equilibrium trajectory. This can be achieved by combining equations (8) and (11). Then v_0 , k and H have to be designed such that σ and ϖ satisfy:

$$\varpi = \frac{1 - \sqrt{1 - \sigma^2}}{\sigma^2} \quad (16)$$

Thus, we can impose the position of the equilibrium trajectory w.r.t. any circle with admissible radius. This naturally leads to the the idea of a better control in the case of an arbitrary curve.

B. Adaptive parameters when tracking an arbitrary target line

The strategy is be to adapt the parameters σ and ϖ dynamically. This gives a great flexibility to this design which can then be modified in function of the needs by adapting on-line the behavior of v_0 , k and H which will then be functions of the time. Among a lot of possibilities, we just give here the extension of the idea presented in the previous paragraph; the goal is to practically stabilize P on the tracked line, with an adaptation of the forward velocity according to the curvature. In fact relation (16) aims at stabilizing P on the osculating circle of the line at the target point, as shown in Fig.9

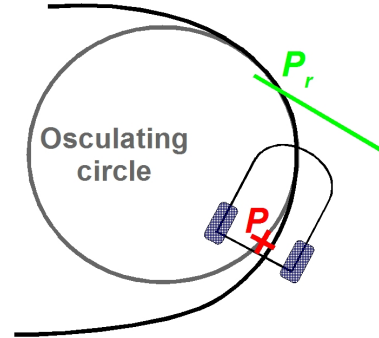


Fig. 9. Practical stabilization of P on the line

Hence, in order to track a curve with an arbitrary shape, we have to compute the line curvature² in real time and perform an on-line adaptation of the design parameters v_0 , k , H so that condition (16) is satisfied for this curvature. Then, if $\frac{dc}{ds}$ is small enough we can consider that P is stabilized on the osculating circle at the target point, which is very close to the line. In addition, we have still one degree of freedom on the parameters so we can choose to increase v_0 in straight lines and decrease it in bends. This last strategy ensures that the transversal acceleration of the robot is not too high, thus, the wheels are prevented from slipping in that direction.

²This can be done by extracting from the image the coordinates of two more points of the line around the target point and computing the curvature of the circle passing through those points; obviously, this requires a more accurate calibration of the image in the neighborhood of the horizon.

C. Experimental results

A simplified version of this adaptive control strategy has been experimentally tested on a target line having the shape represented in Fig.10, including the adaptation of the speed v_0 according to the curvature (faster in straight lines and slower in bends). We report here an experiment with a

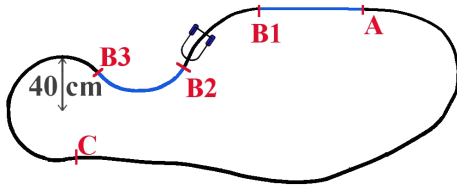


Fig. 10. The test path

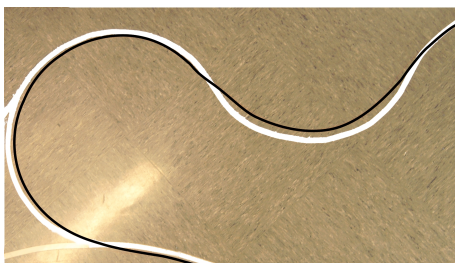


Fig. 11. Approximative motion of P , drawn by a pen attached on the robot

maximum forward velocity of 35cm/s in straight lines. The distance H between the point P and the horizon is about 27 cm. A video of this experiment can be downloaded from <http://www.inma.ucl.ac.be/~coulaud>. As it can be seen, the deviation between P and the target line is kept under 2 cm almost everywhere. The largest deviation observed can be seen on Fig.11, when the robot go through a zigzag. In order to give a more quantitative appreciation of the control behavior, the time evolution of the variable Z during one turn is given in Fig.12. We can see that in the various bends, the behavior is quite similar to that observed in Fig.6 for a circular trajectory.

VI. CONCLUDING REMARKS

We have proposed a simple control design and provided a characterization of the practical domain of stability depending on the parameters of the design and the shape of the line described by its curvature. This analysis has a second important aspect: it makes possible an adaptative design of the parameters of the control law to force the robot to follow the target line as accurately as possible.

The experimental results confirm the analysis and show the robustness of the design in presence of disturbances, as soon as it is used in the conditions mentioned above.

Lots of improvements could be added to the path tracking strategy we propose. Nevertheless, the advantage of our method is that it is really simple to implement and requires few computations for a quite good accuracy of the control compared with the cheapness of the components. Therefore, this control law is adapted for vehicle guidance, provided that the condition of rolling with non-slipping is a good approximation.

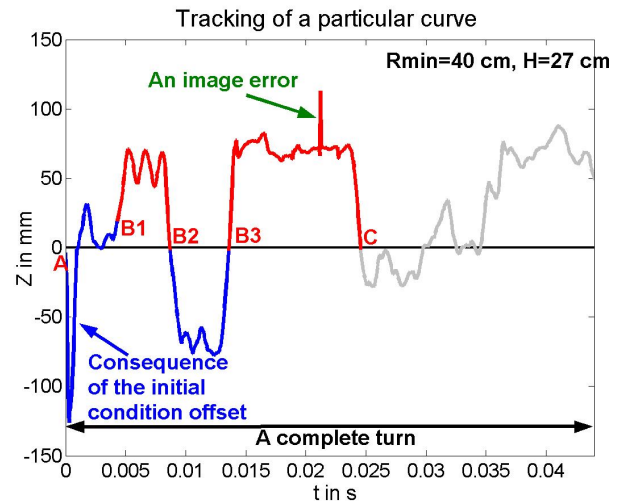


Fig. 12. Evolution of Z when tracking a curve with dynamical parameters

REFERENCES

- [1] A. Broggi, M. Bertozzi, A. Fascioli G. Conte, *Automatic Vehicle Guidance: The Experience of the Argo Autonomous Vehicle*, World Scientific, 1999.
- [2] P.I. Corke, D. Symeonidis, and K. Usher, *Tracking road edges in the panospheric image plane*, IEEE/SRJ Int. Conf. on Intelligent Robots and Systems, pp. 1330–1335, 2003.
- [3] D. Pomerleau, T. Jochem, *Rapidly Adapting Machine Vision for Automated Vehicle Steering*, IEEE Expert **11**, pp. 19-27, 1996.
- [4] C. J. Taylor, J. Košeckà, R. Blasi J. Malik, *A Comparative Study of Vision-Based Lateral Control Strategies for Autonomous Highway Driving*, Int. J. Robot. Res. **18**(5), pp. 442–453, 1999.
- [5] C. Canudas de Wit, B. Siciliano and G. Bastin (Eds), *Theory of Robot Control*, Communications and Control Engineering Series, 1996.
- [6] H. Zhang and J.P. Ostrowski, *Visual motion planning for mobile robots*, IEEE Trans. on Robotics and Automation, pp. 199–208, 2002.
- [7] Y. Masutani, M. Mikawa, N. Maru, and F. Miyazaki, *Visual servoing for non-holonomic mobile robots*, IROS Int. Conf. on Intelligent Robots and Systems, pp. 1133–1140, 1994.
- [8] R. M'Closkey and R. Murray, *Exponential stabilization of driftless nonlinear control systems using homogeneous feedback*, IEEE Trans. on automatic control, vol 42, 1997.
- [9] C. Samson *Control of chained systems: Application to path following and time-varying feedback stabilization*, IEEE Trans. on automatic control, vol 40, 1995.
- [10] O. J. Sørđalen and O. Egeland, *Exponential stabilization of nonholonomic chained systems*, IEEE Trans. on automatic control, vol 40, 1995.
- [11] A. Piazzzi, C.G. Lo Bianco, M. Bertozzi A. Fascioli A. Broggi, *Quintic G2-Splines for the Iterative Steering of Vision-Based Autonomous Vehicles*, Transactions on Intelligent Transportation Systems **3**, pp. 27–36, 2002.
- [12] M. Fliess, J. Lévine, P. Martin P. Rouchon, *A LieBcklund approach to Equivalence and Flatness of Nonlinear Systems*, IEEE Trans. on Automatic Control **44**, pp. 922-937, 1999.
- [13] P. Rouchon, M. Fliess, J. Lévine P. Martin, *Flatness, Motion Planning and Trailer Systems*, Proc. 32nd IEEE Conf. Decision and Control, pp. 2700-2705, 1993.
- [14] Y. Ma, J. Košeckà, S. Sastry, *Vision Guided Navigation for a Nonholonomic Mobile Robot*, IEEE Trans. on Robotics and Automation, 1999.
- [15] H.K. Khalil, *Nonlinear Systems*, pp. 239–246, 2nd ed. Prentice Hall, 1996.